ORIGINAL RESEARCH

Decoration of pH-sensitive copolymer micelles with tumor-specific peptide for enhanced cellular uptake of doxorubicin

Qing Chen[1,*]
Miaomiao Long[2,*]
Lipeng Qiu[3]
Mengqin Zhu[3]
Zhen Li[1]
Mingxi Qiao[1]
Haiyang Hu[1]
Xiuli Zhao[1]
Dawei Chen[1]

[1]Department of Pharmaceutics, School of Pharmacy, Shenyang Pharmaceutical University, Shenyang, [2]Department of Research and Development, Nanjing Chia Tai Tianqing Pharmaceutical Group Co. Ltd, Nanjing, [3]Department of Pharmaceutics, School of Pharmaceutical Sciences, Jiangnan University, Wuxi, People's Republic of China

*These authors contributed equally to this work

Correspondence: Lipeng Qiu
Department of Pharmaceutics, School of Pharmaceutical Sciences, Jiangnan University, 1800 Lihu Avenue, Wuxi 214122, People's Republic of China
Tel +86 510 8519 7769
Fax +86 510 8519 7769
Email flyqlp@163.com

Dawei Chen
Department of Pharmaceutics, School of Pharmacy, Shenyang Pharmaceutical University, 103 Wenhua Road, Shenyang 110016, People's Republic of China
Tel +86 512 6588 4729
Fax +86 512 6588 4729
Email chendawei@syphu.edu.cn

Abstract: To improve the targeting efficacy of hyaluronic acid (HA)-based micelles, pH-sensitive mixed micelles based on HA-g-poly(L-histidine) (PHis) and d-α-tocopheryl polyethylene glycol 2000 copolymers were prepared and decorated with human epidermal growth factor receptor 2 (Her2) peptide, a tumor cell-specific peptide ligand, on their surface. The doxorubicin-loaded micelles (HA-PHis/peptide–d-α-tocopheryl polyethylene glycol 2000 mixed micelles [PHTM]) were characterized to have a unimodal size distribution and pH-dependent drug release pattern. In vitro tumor targeting studies demonstrated that PHTM exhibited the pronounced cytotoxicity and efficient internalization in MDA-MB-231 cells overexpressing CD44 and Her2 receptors. In vivo investigation into micelles in MDA-MB-231 tumor-bearing mice confirmed that PTHM could reach the tumor site more effectively and exert excellent tumor killing activity. In general, Her2 peptide decoration can enhance the selective cytotoxicity and antitumor activity of HA-based micelles.

Keywords: Her2 peptide, hyaluronic acid, poly(L-histidine), targeted delivery, antitumor efficacy

Introduction

The chemotherapeutic drugs used in clinical practice also have some deficiencies, for example, nonspecific toxicity to normal cells, which might result in systemic toxicity, and a low therapeutic efficacy to the host.[1] Development of nanocarrier system has shown promise in enhancing tumor selectivity and decreasing adverse effects of anti-cancer drugs.[2,3] The nanoparticles can perform with hydrophilic surfaces in order to avoid opsonization and removal by the mononuclear phagocytic cells, and they are small enough to take the advantage of the leaky new vasculature and poor lymphatic systems of tumors for accumulation into tumor sites.[4] This phenomenon is known as the enhanced permeability and retention (EPR) effect. As the EPR effect occurs only in solid tumor, the drug-loaded nanovehicles have limited accumulation in normal tissues, leading to reduced side effects of chemotherapy.[5–7]

However, most of the chemotherapeutic drugs act on intracellular pharmacological targets. Although the EPR characteristic increases the distribution of the nanoparticles to the tumor, they cannot readily pass through the cell membrane.[8] The efficacy of anticancer drugs can be further enhanced by facilitating the intracellular uptake with specific affinity of the nanoparticles for the cancer cells.[8–10] Therefore, active target-ing of the nanoparticles modified with binding ligands may be more favorable. To achieve receptor-mediated targeting, various targeting moieties including peptides,

antibodies, proteins, aptamers, sugars, and small molecules, which bind to the tumor-specific receptors, are conjugated to the nanoparticle surface for enhanced cellular delivery of nanoparticles.[7,11,12]

Antibodies are used as tumor-binding ligands because of high specificity and affinity.[13,14] However, certain limitations, such as poor solubility, expensiveness, immune response, poor stability, and little tumor penetration, hamper the efficient development of antibodies in drug delivery devices.[15] Therefore, more fruitful alternatives to antibodies are explored, and easy-to-manufacture antibody mimics attract recent interest.[16–18] The antibody mimics are usually tumor-specific peptides that possess the essential molecular recognition features of antibody. The smaller size of peptides has better tumor cell penetration, and the progress of peptide synthesis and engineering is more conducive to drug development.[19]

The human epidermal growth factor receptor 2 (Her2) is a member of the ErbB family of receptor tyrosine kinases, which is amplified in ~30% of breast cancers and 20% of ovarian cancers, but it is amplified weakly in normal tissues.[20–22] The receptor comprises an extracellular ligand-binding domain that is easily accessed by Her2 ligands; therefore, it can be considered as an attractive marker for active targeted delivery to tumor cells.[23,24] Her2 cyclic peptide is a novel analog of trastuzumab (Herceptin®), which is the only Her2-targeted therapy approved by US Food and Drug Administration for the treatment of breast cancer, and it can specifically recognize the Her2 receptor with low concentrations.[25]

In a previous work, a pH-sensitive micellar delivery system based on the hyaluronic acid-g-poly(L-histidine) (HA-PHis) copolymers was reported. HA is a biodegradable polyanionic polysaccharide and a ligand for CD44 receptor overexpressed in a variety of tumor cells.[26,27] PHis is a pH-sensitive actuator with endolysosomal escape nature.[28] The HA-PHis copolymer-based micelles provide an effective approach for increasing cellular uptake and rapid delivery of doxorubicin (DOX) into the cytosol, resulting in significant increases in therapeutic efficacy.[29] Then, d-α-tocopheryl polyethylene glycol 2000 (TPGS2k) amphiphilic polymer was introduced to develop the mixed copolymer micelles for delivering DOX into drug-resistant breast cancer cells.[30]

Although the aforementioned HA-based micelles significantly improve the intracellular delivery of DOX, they enter the tumor cells just relying on the CD44 receptor-mediated active targeting. However, it has been reported that

CD44 receptors have some disadvantages, such as intrinsic variability and easy saturation, which cause a relatively low capacity of receptor-mediated uptake.[31,32] Furthermore, except for CD44 receptors, HA receptors such as HARE and LYVE1 are expressed in endothelial cells in liver and lymphatic system.[33–36] Therefore, more modifications in HA should be proceeded to enhance the targeting ability and reduce the accumulation in the normal organs.

Her2 has been identified as an important molecular marker in breast cancer,[20,37] and it has become a therapeutic target in clinical practice.[38,39] With the development of drug delivery system, Her2 receptor-mediated cellular uptake has attracted substantial interest in targeted drug delivery. Therefore, Her2 peptide was functionalized to the mixed micelles composed of HA-PHis and TPGS2k copolymers, aiming to obtain precise dual-targeting efficacy and extensive penetration into breast tumor. The pH-sensitive dual-targeting micelles can be accumulated at the tumor tissue by the EPR effect and selectively taken up into the tumor cells through both CD44 receptor- and Her2 receptor-mediated endocytosis. Then, the micelles disassemble rapidly in the acidic endolysosomes due to pH-induced protonation of PHis block, resulting in the drug burst release into cytoplasm. By using DOX as the model drug, the targeting characteristics of the dual-targeting HA-based micellar system were evaluated in vitro and in vivo.

Materials and methods
Materials
The HA-PHis was synthesized according to the previously reported procedures. D-α-tocopheryl acid succinate was obtained from Jiangsu Xixin International Co., Ltd. (Suqian, People's Republic of China). Methoxyl PEG2000-amine (mPEG2k-NH$_2$) and amine-PEG2000-carboxymethyl (NH$_2$-PEG2k-COOH) were bought from Yare Biotech (Shanghai, People's Republic of China). Her2 peptide (YCDGFYA-CYMDV, Figure 1A) was synthesized by China Peptides Co., Ltd. (Shanghai, People's Republic of China). DOX hydrochloride was purchased from Huafeng United Technology (Beijing, People's Republic of China). N-hydroxysuccinimide (NHS) and 1-ethyl-3-(3-dimethylaminopropyl) carbodiimide (EDC) were obtained from Sinopharm Chemical Reagent Co., Ltd. (Shanghai, People's Republic of China), and 3-(4,5-dimethylthiazol-2-yl)-2,5-diphenyl tetrazolium bromide (MTT) and Hoechst 33342 were bought from Beyotime (Shanghai, People's Republic of China). Dulbecco's Modified Eagle's Medium (DMEM), Roswell Park Memorial
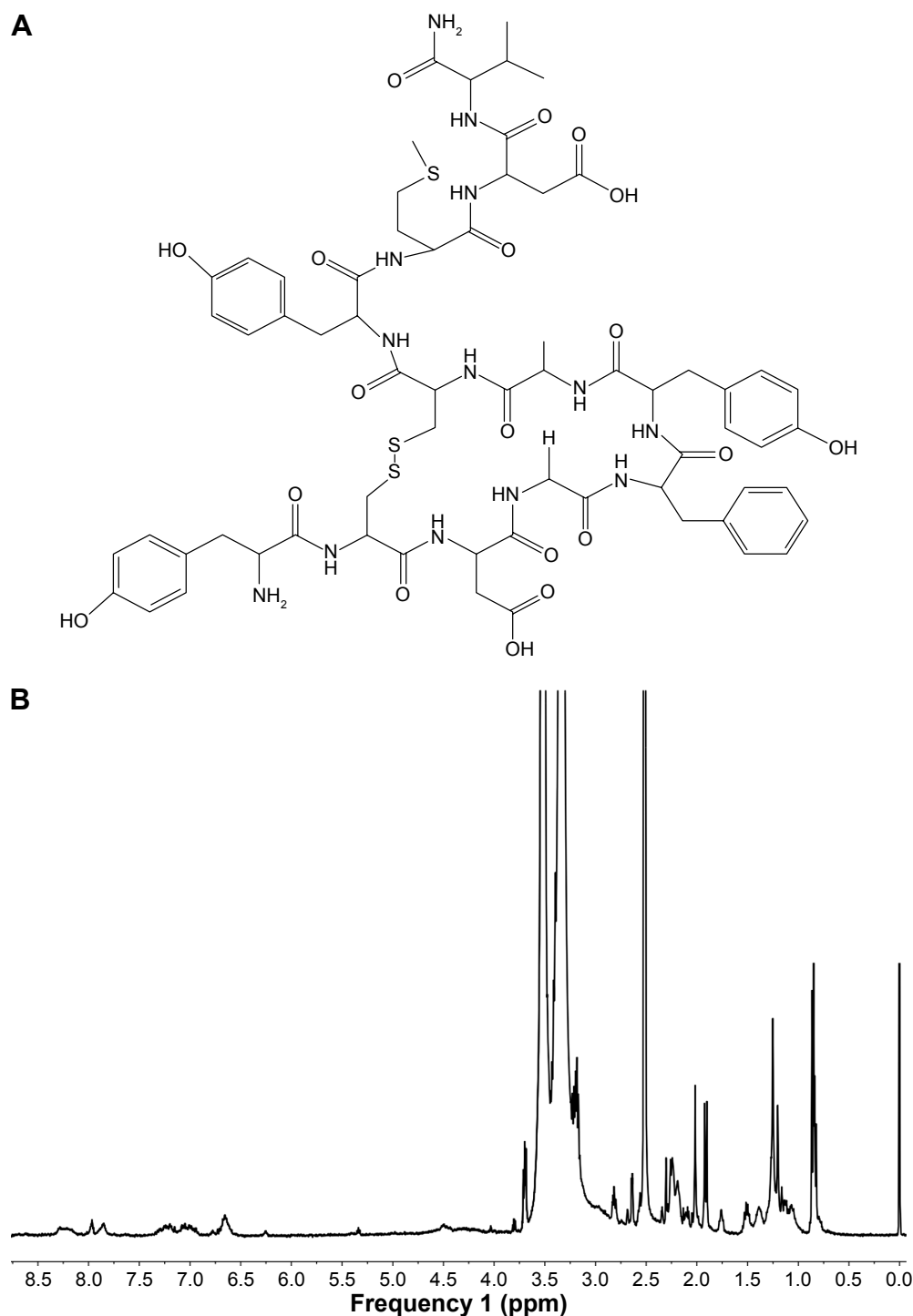
A

B

Figure 1 (**A**) Chemical structure of Her2 peptide and (**B**) ^{1}H NMR spectrum of pep-TPGS2k in DMSO-d6.
Abbreviations: d6, ^{1}H NMR spectrum; DMSO, dimethyl sulfoxide; ^{1}H NMR, proton nuclear magnetic resonance; TPGS2k, d-α-tocopheryl polyethylene glycol 2000; pep-TPGS2k, Her2 peptide-modified TPGS2k.

Institute (RPMI)-1640 medium, fetal bovine serum (FBS), and penicillin–streptomycin solution were purchased from Gibco® BRL (Thermo Fisher Scientific, Waltham, MA, USA). All the other chemicals and buffer solution components were analytical-grade preparations.

Cell cultures

Human breast cancer cell line MCF-7 and MDA-MB-231 cells were obtained from Chinese Academy of Sciences (Shanghai, People's Republic of China). They were cultured in DMEM supplemented with 10% FBS and 1% penicillin–streptomycin

solution. All cells were cultured at 37°C in a humidified atmosphere with 5% CO_2. This study and the study protocol were approved by the medical ethics committee of the First Affiliated Hospital of Soochow University.

Synthesis of Her2 peptide-modified TPGS2k

TPGS2k was synthesized as described in a previous report.[30] Her2 peptide-modified TPGS2k (pep-TPGS2k) was executed by a two-step reaction. First, HOOC-TPGS2k was synthesized by the same procedures as those of TPGS2k, except that NH_2-PEG-COOH was used in this reaction. Second, equimolar Her2 peptide was added to HOOC-TPGS2k solution, which was activated beforehand by EDC and NHS with stoichiometric ratio of 1:2:2. Then, the mixture was stirred at a room temperature under a nitrogen atmosphere for 48 h. After centrifugation 4 times at 5,000 rpm for 30 min by a tubular ultrafiltration membrane (molecular weight cutoff [MWCO] 3000) and then dialysis (MWCO 3000) against 1,000 mL deionized water for 3 days to remove the uncoupled peptide, the solution was lyophilized to obtain pep-TPGS2k polymer. The structure of pep-TPGS2k was confirmed by proton nuclear magnetic resonance (^{1}H NMR) spectrometry (400 MHz; Varian, PaloAlto, CA, USA).

The conjugation efficiency of peptide with the pep-TPGS2k was assessed using the Micro Bicinchoninic Acid Protein Assay Kit (Beyotime, Shanghai, People's Republic of China), which provided a rapid and sensitive method for the quantitation of peptides and proteins.[19,40,41] The concentration of the peptide was calculated on the basis of a calibration curve of $y=2.2787x+215.75$ ($r=0.9993$), and the conjugation efficiency was 11.75%±2.31%.

Preparation and characterization of DOX-loaded copolymer micelles

DOX-loaded HA-PHis/pep-TPGS2k mixed micelles (PHTM) were prepared by using the ultrasonication method (JY92-II; Ningbo, People's Republic of China). Next, 10 mg HA-PHis and 2 mg pep-TPGS2k were dispersed in 10 mL PBS (0.1 M, pH 7.4), and 2 mg DOX was dissolved in tetrahydrofuran/acetone (1:1, v/v). Then, the DOX solution was added dropwise into the copolymer solution with stirring at room temperature. After stirring for 12 h in order to remove the solvent, the mixture was ultrasonicated for 30 min (active every 2 s for a 3-s duration with an output power of 100 W) in ice bath. Then, the micellar suspension was filtered through a membrane filter (0.45 μm) to remove insoluble drug and centrifuged 3 times at 5,200 rpm for 30 min by a tubular ultrafiltration membrane (MWCO 3000; Millipore,

Suzhou, People's Republic of China) to remove free drug. The DOX-loaded HA-PHis/TPGS2k mixed micelles (HTM) and the corresponding blank mixed micelles were prepared in the same way.

The size and ζ-potential of the micelles were measured by using a Zeta Potential/Particle Sizer Nicomp™ 380ZLS (PSS Nicomp, Santa Barbara, CA, USA). The micellar suspensions were placed on copper grids with films, air-dried for 10 min, and finally examined by transmission electron microscopy (TEM; Tecnai G220, FEI, Hillsboro, OR, USA) to visualize the morphology of copolymer micelles.

The drug loading (DL) and encapsulation efficiency (EE) of copolymer micelles were measured by ultraviolet (UV) spectrophotometry. Briefly, DOX-loaded micellar solution was diluted 10-fold with formylamine and then ultrasonicated for 10 min to disrupt the assembled micelles and dissolve drugs. The DOX content was analyzed with a UV spectrophotometer (UV-2600, Shimadzu, Japan) at 479 nm. DL and EE were calculated as the ratio of the drug weight in the micelles to the total weight of the micelles and feeding weight of drug, respectively.

In vitro pH-sensitive release

The release profiles of DOX from the mixed micelles were investigated by the dynamic dialysis method; 2.0 mL DOX-loaded micelles was introduced into a dialysis bag (MWCO 3500 Da) and then immersed in 20 mL fresh PBS solution (pH 5.0 and 7.4, 0.1 M) in a vial that was placed in a shaking incubator at a stirring speed of 100 rpm at 37°C. Aliquots of medium (1.0 mL) was collected at determined times (1, 2, 4, 6, 8, 12, and 24 h) and replaced with an equivalent volume of fresh medium (37°C). The concentration of DOX released from the mixed micelles was measured with a UV/visible spectrophotometer as described previously.

In vitro cytotoxicity tests

MCF-7 cells and MDA-MB-231 cells were adopted to evaluate the cytotoxicity of blank mixed micelles and DOX-loaded mixed micelles. CD44 receptors are overexpressed in both the cells, but Her2 receptors are more expressed in MDA-MB-231 cells than in MCF-7 cells. The cells were seeded at the density of 7×10^3 cells/well in 96-well plates and incubated for 24 h to allow cell attachment. Then, the cells were incubated with blank micelles, DOX-loaded micelles, and free DOX for 48 h in a concentration gradient at 37°C. Later, 10 μL of MTT (5 mg/mL) was added to the medium and further incubated for 4 h. The medium in each well was removed, and 100 μL of dimethyl sulfoxide (DMSO) was added to dissolve the internalized purple formazan crystals.

The absorbance at 492 nm was recorded using a BioRed microplate reader (MK3, Thermo Fisher Scientific). The sensitivity of tumor cells to HTM, PHTM, or free DOX was measured by the concentration inducing 50% loss of cell viability (IC_{50}).

Cellular uptake studies

The cellular uptake efficiency was evaluated quantitatively by using flow cytometry. MDA-MB-231 and MCF-7 cells were seeded on a 6-well culture plate with a density of 3×10^4 cells/well for 24 h. Free DOX or DOX-loaded micelles with equivalent DOX concentration (5.0 μg/mL) were added and incubated for 1 and 4 h. Then, the cells were washed 3 times with ice-cold PBS (pH 7.4), harvested, and subsequently resuspended in 0.5 mL PBS for analysis by using a flow cytometer (FACSCalibur™, BD Biosciences, San Jose, CA, USA).

Cellular uptake and distribution of DOX from developed micelles were also observed by confocal laser scanning microscopy (CLSM). After MDA-MB-231 cells achieved 80% confluency, the cells were seeded on microscope slides in a 6-well plate at a density of 1×10^4 cells/well and incubated for 24 h at 37°C. DOX (5.0 μg/mL), alone or entrapped in the mixed micelles, was added and incubated for 1 and 4 h. After incubation, all the reagents were removed, and Hoechst 33342 (10 μg/mL) was used to visualize the nuclei. The cells were washed at least 3 times with PBS and fixed with 5% paraformaldehyde solution for 15 min, and then, they were observed by CLSM (LSM710, Carl Zeiss Meditec AG, Jena, Germany).

Mechanisms of cellular uptake

MDA-MB-231 cells were seeded in 6-well plates at a density of 5×10^5 cells/well and incubated for 24 h at 37°C. After incubating with 10 μg/mL chlorpromazine (CPM), 40 μg/mL colchicines (CC), 5 μg/mL filipin (FLP), 10 mg/mL pep, 10 mg/mL HA, or the mixture of pep and HA (1:1, v/v) for 30 min, PHTM (5.0 μg/mL of DOX) was added and incubated for a further 4 h. Then, cells were washed and harvested for analysis by using a flow cytometer. The cells were incubated without uptake inhibitor as controls.

In vivo imaging analysis of mixed micelles

Female BALB/c nude mice (5–6 weeks of age) were purchased from SLAC Laboratory Animal Co., Ltd. (Shanghai, People's Republic of China) and were used to generate the tumor xenograft mouse model. Mice were housed at 25°C and allowed free access to food and water. All animal procedures were performed following the protocol approved by the Institutional Animal Care/User Ethical Committee of Soochow University.

The MDA-MB-231 cells (1×10^7 cells in 0.1 mL of cell culture medium) were injected subcutaneously into the abdomen of the mice. 1,1′-Dioctadecyl-3,3,3′,3′-tetramethylindotricarbocyanine (DIR)-loaded HTM and PHTM with equal fluorescence were injected into the tail vein of the tumor xenograft mice when the tumor volume reached ~100–200 mm³. At 6, 12, 24, and 48 h postinjection, the tumor accumulation profiles were assessed by using a near-infrared (NIR) fluorescence imaging system (IVIS Lumina, Caliper, Princeton, NJ, USA). The mice under anesthetic state via inhalation of isoflurane were automatically moved into the imaging chamber for scanning. Finally, they were sacrificed, and the major organs and tumors were dissected from the mice 48 h after intravenous injection. Each organ and tumor was rinsed with physiological saline for 3 times followed by the capture of fluorescent images.

In vivo antitumor efficacy test

Female BALB/c nude mice were inoculated subcutaneously with MDA-MB-231 cells (1×10^6 cells in 0.1 mL of cell culture medium) in the abdomen. Tumors were allowed to grow to ~100 mm³ before treatment, and the mice were randomly divided into 4 groups (n=5). The tumor size was measured with Vernier calipers every day, and tumor volume (mm³) was calculated using the formula: volume $=0.5\times LW^2$ (L is the long diameter, and W is the short diameter of a tumor). Experimental groups were as follows: saline, DOX solution, HTM, and PHTM (10 mg/kg dose). Each group was injected by tail vein every 72 h for 3 times. After the final administration, the mice were further observed for 3 days, and then, the tumors were harvested and weighed. The tumor volumes and body weights of the mice were all measured in this process.

Statistical analysis

Statistical analysis was performed by using one-way analysis of variance, and $P<0.05$ was considered statistically significant. All the experiments were performed at least 3 times, and the data were represented as the mean ± standard deviation.

Results and discussion
Synthesis and characterization of pep-TPGS2k

Her2 peptide was conjugated to the terminal of TPGS2k through a reaction between the carboxyl group of PEG and

the amino group of the Her2 peptide. Figure 1B shows a typical ^{1}H NMR spectrum (DMSO-d6) of pep-TPGS2k. The peaks at δ 0.83 ppm ($-CH(C\underline{H}_3)_2-$) and δ 1.892–2.01 ppm ($-C\underline{H}_3$ on phenyl group) of VES, the characteristic peak at δ 3.51 ppm ($-OC\underline{H}_2C\underline{H}_2O-$) of PEG chain, and the distinctive peaks at δ 6.65–7.19 ppm ($Ar-C\underline{H}-$) and δ 7.81–8.27 ppm ($-CO-N\underline{H}-$) of Her2 peptide all appeared in the spectrum, indicating that pep-TPGS2k was successfully synthesized.

Preparation and characterization of the micelles

The uniform mixed micelles composed of HA-PHis and TPGS2k were formed in a previous study.[30] Her2 peptide-modified micelles were prepared by using the same method with the addition of pep-TPGS2k. Table 1 summarized the average particle sizes, polydispersity index, zeta potentials, and EE and DL of the DOX-loaded micelles. The relatively narrow size distribution of the micelles indicated the formation of the uniform disperse mixed micelles (Figure 2A).[42] The moderate negative zeta potentials resulting from the ionized carboxylic group of HA in the shell may prevent the aggregation of micelles through electrostatic repulsion. As shown in Figure 2B, TEM showed that the PHTM had a nearly spherical morphology and good dispersion. In addition, DL and EE of PHTM were similar to those of HTM, which suggested that modification in Her2 peptide played a negligible role in the accommodation of DOX in the micelles.

In vitro release of DOX from the micelles

The pH-sensitive drug release behaviors of the micelles were investigated at endolysosomal pH (~5.0) and physiological pH (~7.4). As shown in Figure 3A, a significant difference was found in the DOX release from PHTM at different pH values ($P<0.05$), which presented the similar release profiles of the previous HTM and HA-PHis micelles. The different release behavior of the micelles was attributed to the physical destabilization of the hydrophobic core of HA-PHis-based micelles at various pH values. The micelles had more compact hydrophobic micellar core composed of unprotonated PHis at pH 7.4, resulting in sustained release of DOX. When the pH decreased below 5.0, the protonated PHis

blocks started to repel each other due to the same electrical charge, leading to the swelling of micellar core and triggering the DOX release.[43,44] Therefore, it can be concluded that DOX was released slowly under a physiological condition, while a quick release was taken place at the acidic tumor environment for efficiently killing the tumor cells.

In vitro cytotoxicity studies

In vitro cytotoxicity of DOX, HTM, and PHTM was tested against MCF-7 cells and MDA-MB-231 cells. As shown in Figure 3B, HTM and PHTM showed significant higher cytotoxicity than free DOX ($P<0.05$). The IC$_{50}$ values of HTM and PHTM were similar in MCF-7 cells ($P>0.05$), indicating that there was no significant difference of cytotoxicity between HTM and PHTM. However, in MDA-MB-321 cells, the IC$_{50}$ value of PHTM was lower than that of HTM ($P<0.05$), which suggested that PHTM existed the highest cytotoxicity in all formulations. These results could be explained that the CD44 receptors that mediate HA-based copolymer micelles entering cells quickly are overexpressed in both MCF-7 cells and MDA-MB-231 cells. Meanwhile, MDA-MB-231 cells express more Her-2 receptors than MCF-7 cells, resulting in more effective uptake of PHTM into the cells. Therefore, PHTM modified with Her2 peptide had the enhanced cytotoxicity.

In vitro cellular uptake studies

The cellular uptake of DOX after incubation with different formulations was evaluated by flow cytometry. As shown in Figure 4, the intracellular uptake of all preparations in MCF-7 and MDA-MB-231 cells showed a time-dependent manner, and the amount of DOX after 4-h incubation was larger than that after 1-h incubation ($P<0.05$). In the two kinds of cells, the intracellular accumulation of free DOX was lower than that of DOX-loaded mixed micelles at different times, which coincided with the result of cytotoxicity test. There was no significant difference in DOX accumulation by MCF-7 cells from the mixed micelles at various times ($P>0.05$), suggesting that the recognition of CD44 receptors and pH-sensitive micellar core of the mixed micelles were not influenced by the Her2 peptide. However, although both

Table 1 Characterization of HTM and PHTM copolymer micelles

Copolymer micelles	Mean diameter (nm)	Polydispersity	Zeta potential (mV)	EE (%)	LC (%)
HTM	159.9±4.5	0.112±0.032	−14.4±1.32	91.7±1.98	10.8±0.36
PHTM	169.8±11.0	0.066±0.047	−12.3±0.98	93.1±1.45	10.0±0.88

Abbreviations: EE, encapsulation efficiency; HA, hyaluronic acid; HTM, HA-PHis/TPGS2k mixed micelles; LC, drug loading content; PHis, poly(L-histidine); PHTM, HA-PHis/pep-TPGS2k mixed micelles; pep-TPGS2k, Her2 peptide-modified TPGS2k; TPGS2k, d-α-tocopheryl polyethylene glycol 2000.

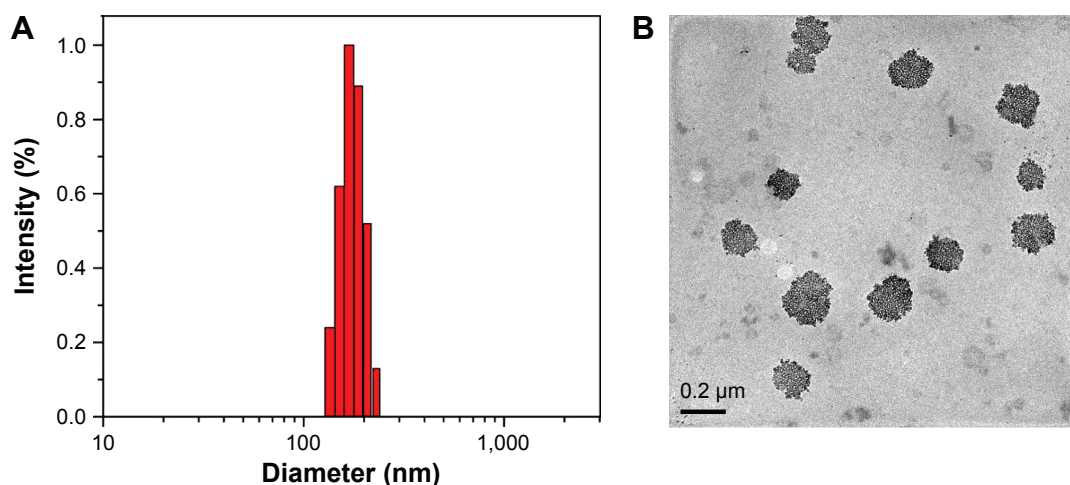**Figure 2** (**A**) Particle size distribution and (**B**) TEM image of PHTM micelles.
Abbreviations: HA, hyaluronic acid; PHis, poly(L-histidine); PHTM, HA-PHis/pep-TPGS2k mixed micelles; pep-TPGS2k, Her2 peptide-modified TPGS2k; TEM, transmission electron microscopy; TPGS2k, d-α-tocopheryl polyethylene glycol 2000.

of the mixed micelles had the close amount of DOX after 1-h incubation in MDA-MB-231 cells, PHTM showed 1.3-fold higher uptake efficiency of DOX than HTM ($P<0.05$) after 4-h incubation. With the prolonging incubation time, the uptake efficiency of PHTM was enhanced due to the receptor-mediated endocytosis in MDA-MB-231 cells with more Her2 receptors. The higher uptake efficiency of PHTM than HTM indicated that the synergistic effect of dual-receptor-mediated endocytosis could generate more internalization of HA-based micelles.

To further evaluate the intracellular uptake efficiency, CLSM was used to identify the location of the DOX in MDA-MB-231 cells. Figure 5 shows the fluorescence microscope images of MDA-MB-231 cells after 1 and 4 h of incubation with free DOX, HTM, and PHTM. For all the formulations, the fluorescence intensities were increased obviously with the extension of incubation time. Compared with free DOX, the more intracellular accumulation of HTM and PHTM was caused by receptor-mediated endocytosis and pH-triggered release. However, the fluorescence intensity of PHTM was stronger than that of HTM after a 4-h incubation, and DOX was mainly distributed in the nucleus. These results were consistent with the fact that the enhanced cellular uptake of PHTM was attributed to not only the interaction between HA and CD44 receptors but also the interaction between peptide and Her2 receptors.
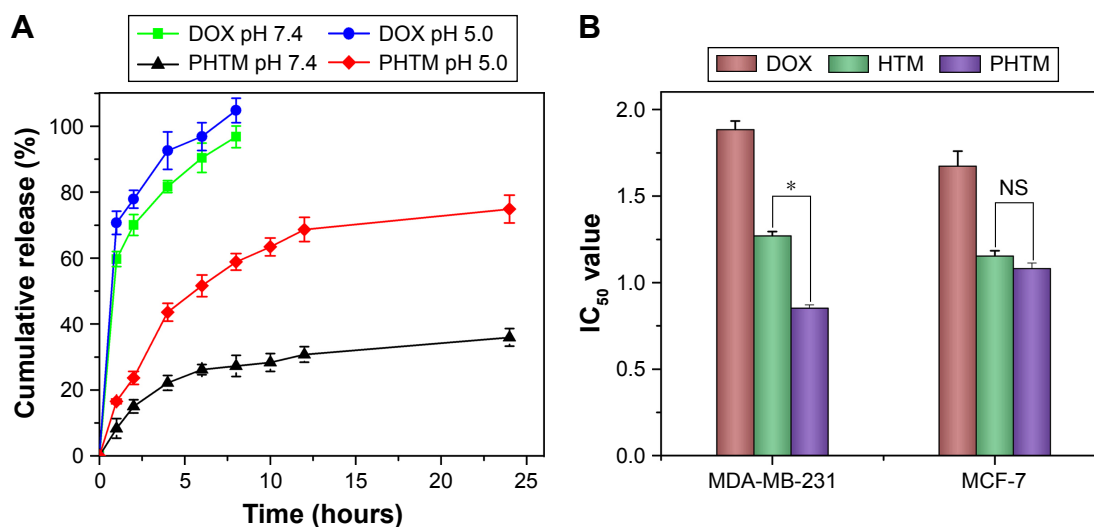

Figure 3 (**A**) pH-dependent release of DOX from PHTM and HTM at 37°C and (**B**) cytotoxicity of free DOX, HTM, and PHTM against MCF-7 and MDA-MB-231 cells.
Notes: Data expressed as mean ± standard deviation (n=3). *$P<0.05$.
Abbreviations: DOX, doxorubicin; HA, hyaluronic acid; HTM, HA-PHis/TPGS2k mixed micelles; IC$_{50}$, concentration inducing 50% loss of cell viability; NS, not significant; pep-TPGS2k, Her2 peptide-modified TPGS2k; PHis, poly(L-histidine); PHTM, HA-PHis/pep-TPGS2k mixed micelles; TPGS2k, d-α-tocopheryl polyethylene glycol 2000.
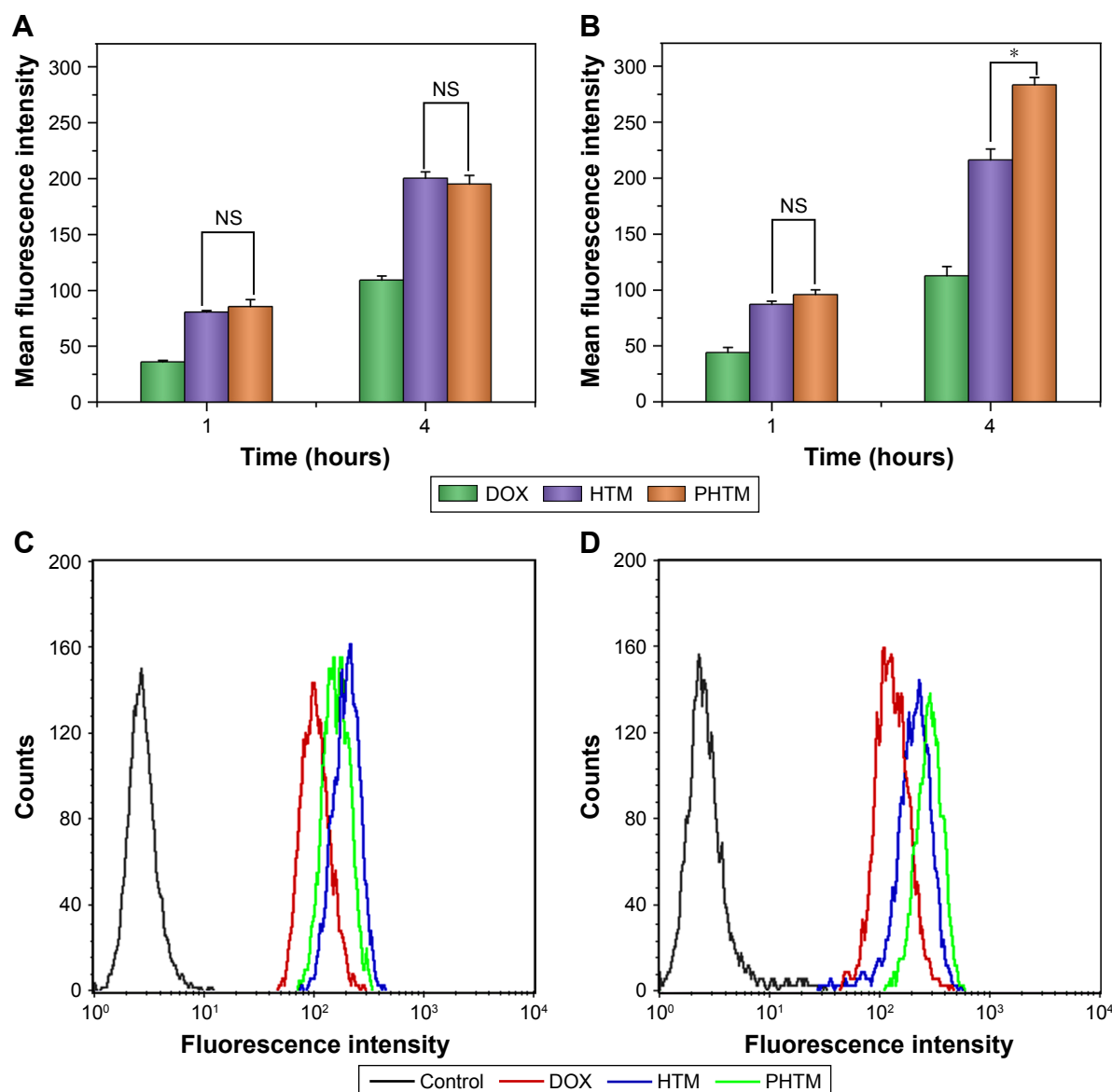
Figure 4 Flow cytometry measurement of the intracellular uptake of free DOX, HTM, and PHTM in MCF-7 cells (**A**) and MDA-MB-231 cells (**B**) and the fluorescence intensity of DOX accumulation at 4 hours in MCF-7 cells (**C**) and MDA-MB-231 cells (**D**), respectively.

Notes: *$P<0.05$. Data expressed as mean ± standard deviation (n=3).

Abbreviations: DOX, doxorubicin; HA, hyaluronic acid; HTM, HA-PHis/TPGS2k mixed micelles; NS, not significant; pep-TPGS2k, Her2 peptide-modified TPGS2k; PHis, poly(L-histidine); PHTM, HA-PHis/pep-TPGS2k mixed micelles; TPGS2k, d-α-tocopheryl polyethylene glycol 2000.

Mechanisms of cellular uptake

To elucidate the potential cellular uptake pathways of PHTM, CPM, FLP, and CC were chosen as uptake inhibitors, and HA, Her-2 pep, and mixtures of them were used as CD44 receptors and Her-2 receptors competitive inhibitors, respectively. First, the cytotoxicity of various inhibitors was evaluated. As shown in Figure 6A, the cell viabilities exceeded 90%, indicating that the inhibitors with the used concentration were nontoxic to the cells.

The results of internalization of PHTM in the presence of different inhibitors are shown in Figure 6B and C.

Compared with the control group, the cellular uptakes of micelles were reduced to 70.8% and 39.5% ($P<0.05$) in the presence of Her2 peptide and HA, respectively. Moreover, the amount of internalization was observably reduced to 26.2% ($P<0.05$) after incubation with the mixture of HA and peptide. These results suggested that the competitive binding of CD44 and Her2 receptors could reduce the cellular uptake of PHTM via receptor-mediated endocytosis. CC was used to evaluate the effect of the macropinocytosis pathway on the uptake of micelles, and no significant difference ($P>0.05$) was presented compared with the control, implying that
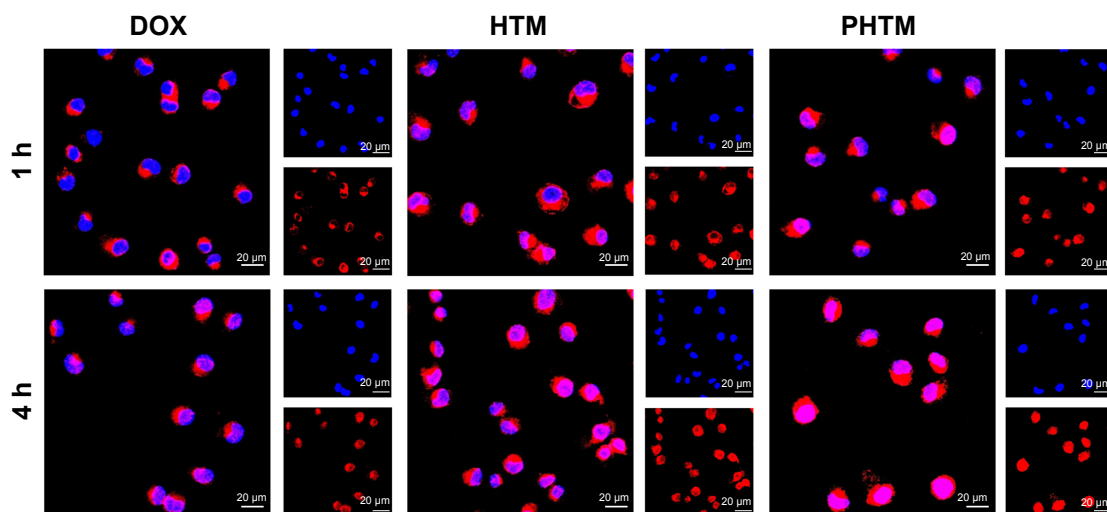
Figure 5 CLSM images of MDA-MB-231 cells after 1 h and 4 h of incubation with free DOX, HTM, and PHTM.
Abbreviations: CLSM, confocal laser scanning microscopy; DOX, doxorubicin; h, hours; HA, hyaluronic acid; HTM, HA-PHis/TPGS2k mixed micelles; pep-TPGS2k, Her2 peptide-modified TPGS2k; PHis, poly(L-histidine); PHTM, HA-PHis/pep-TPGS2k mixed micelles; TPGS2k, d-α-tocopheryl polyethylene glycol 2000.
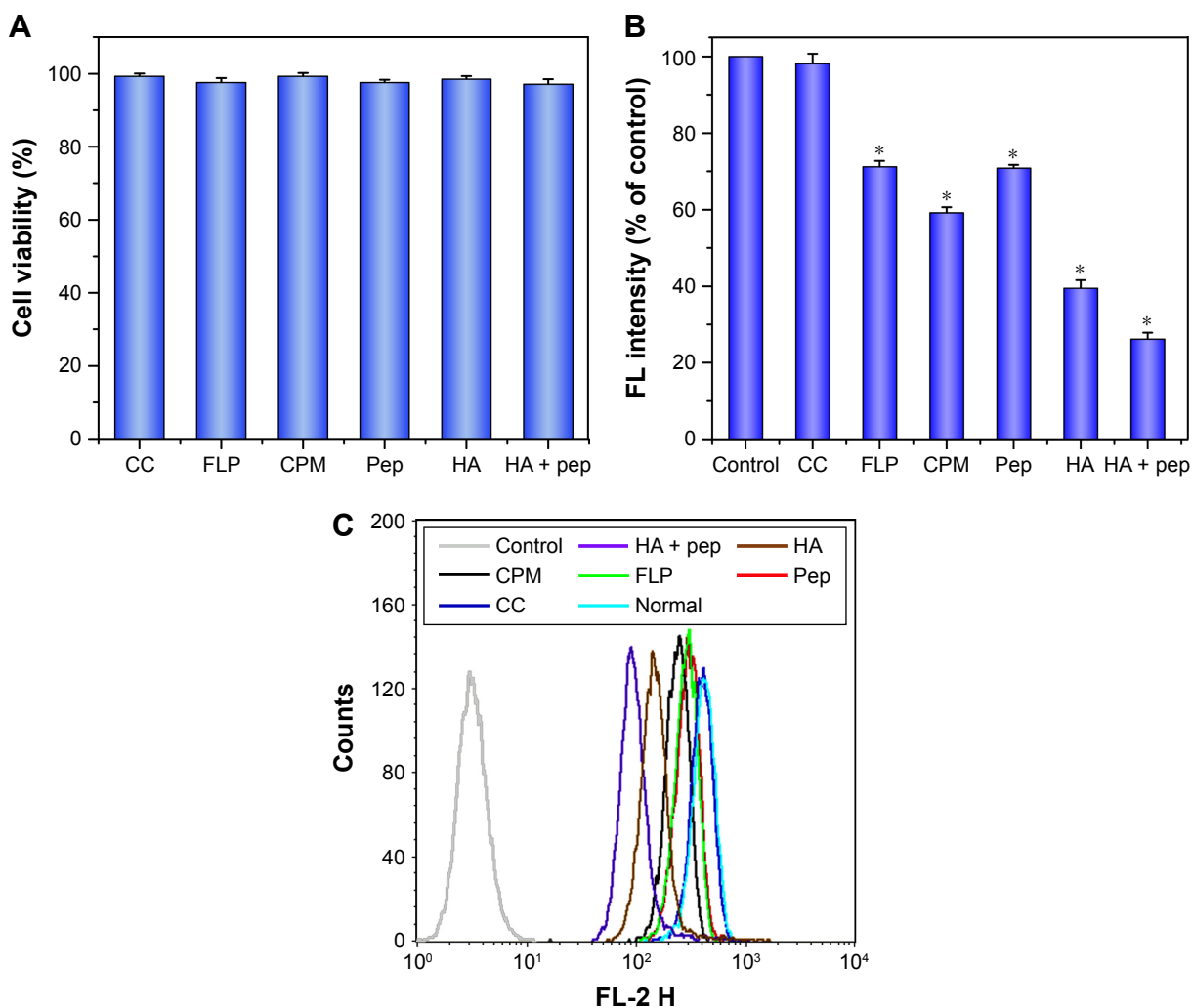

Figure 6 (**A**) In vitro viability of MDA-MB-231 cells treated with different inhibitors and (**B** and **C**) the effects of inhibitors on the uptake of PHTM in MDA-MB-231 cells.
Notes: Data expressed as mean ± standard deviation (n=3). *$P<0.05$.
Abbreviations: CC, colchicines; CPM, chlorpromazine; FLP, filipin; HA, hyaluronic acid; PHis, poly(L-histidine); pep, Her2 peptide; pep-TPGS2k, Her2 peptide-modified TPGS2k; PHTM, HA-PHis/pep-TPGS2k mixed micelles; TPGS2k, d-α-tocopheryl polyethylene glycol 2000.

macropinocytosis was not closely involved in the internalization of micelles. However, in the presence of CPM and FLP (clathrin-mediated pathway inhibitor and caveolae-mediated pathway inhibitor, respectively), the cellular uptake of micelles was reduced to 59.2% and 71.2% ($P<0.05$), which suggested that the clathrin- and caveolae-mediated pathways were both involved in the uptake of PHTM. These results are consistent with our previous research,[29] indicating that the uptake routes of HA-PHis-based micelles modified with Her2 peptide are not significantly changed.

In vivo imaging analysis

In vivo real-time biodistribution and tumor target of the PHTM in MDA-MB-231 tumor-bearing mice were evaluated through noninvasive NIR optical imaging technique. DIR was chosen as a fluorescent marker. The diagnosis profiles of the mixed copolymer micelles were clearly visualized by monitoring real-time NIR fluorescence intensity at 6, 12, 24, and 48 h after being injected intravenously with the polymer micelles. As shown in Figure 7A, both the micelles had a time-dependent biodistribution and tumor accumulation in the mice, and most of the DIR accumulated in liver and tumor. With the prolongation of time, the fluorescence intensity in the tumor region was increased, which could be mainly due to the receptor-mediated uptake of micelles.[45] However, the fluorescence intensity of the PHTM in the tumor region was stronger than that of the HTM after 12-h administration, suggesting that dual-receptor-mediated endocytosis could enhance the accumulation of HA-based micelles.

Furthermore, the major organs and tumor tissues were isolated and studied (Figure 7B). Except that the fluorescence signals were shown in livers and spleens resulting from reticuloendothelial system,[46] the other organs, especially the hearts, were not observed fluorescence signals. This indicated that the mixed micelles could effectively reduce the cardiotoxicity induced by DOX. As anticipated, the PHTM showed stronger fluorescence intensity (1.76-fold) in tumor tissue than HTM ($P<0.05$; Figure 7C). These results indicate that Her2 peptide-modified HA-based micelles can improve the accumulation of anticancer drugs in the tumors.

In vivo antitumor efficacy of PHTM

To investigate the in vivo antitumor activity of PHTM, the tumor volume of the tumor-bearing mice was monitored. As shown in Figure 8A, the control group treated with saline showed rapid increase in the tumor volume, whereas other groups observably inhibited the tumor growth ($P<0.05$). Compared with HTM-treated group, the antitumor efficacy was higher in PHTM-treated groups ($P<0.05$), primarily ascribed to high tumor target ability of Her2 peptide-modified micelles. In addition, the body weight of the mice treated with the micelles was not significantly changed (Figure 8B). However, the mice treated with free DOX exhibited clear weight loss, which might be attributed to the severe side effect of DOX as previously reported.[47,48] Furthermore, the smallest tumors were shown in PHTM-treated group (Figure 8C), and the average tumor weight in the group of PHTM was 2.31-fold lower than that of free DOX and 1.69-fold lower
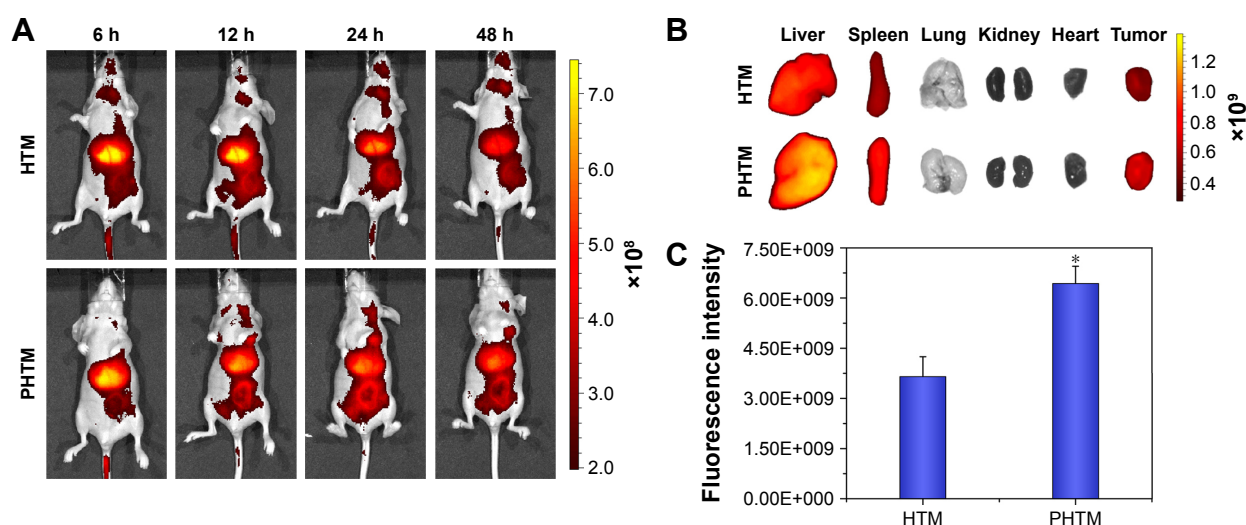

Figure 7 (**A**) In vivo noninvasive images of time-dependent whole body imaging of MDA-MB-231 tumor-bearing mice after injection of HTM and PHTM; (**B**) ex vivo optical images of tumors and organs; and (**C**) the fluorescence intensity in the tumor region of MDA-MB-231 tumor-bearing mice sacrificed at 48 h (n=3).
Note: *$P<0.05$.
Abbreviations: h, hours; HA, hyaluronic acid; HTM, HA-PHis/TPGS2k mixed micelles; PHis, poly(L-histidine); pep-TPGS2k, Her2 peptide-modified TPGS2k; PHTM, HA-PHis/pep-TPGS2k mixed micelles; TPGS2k, d-α-tocopheryl polyethylene glycol 2000.
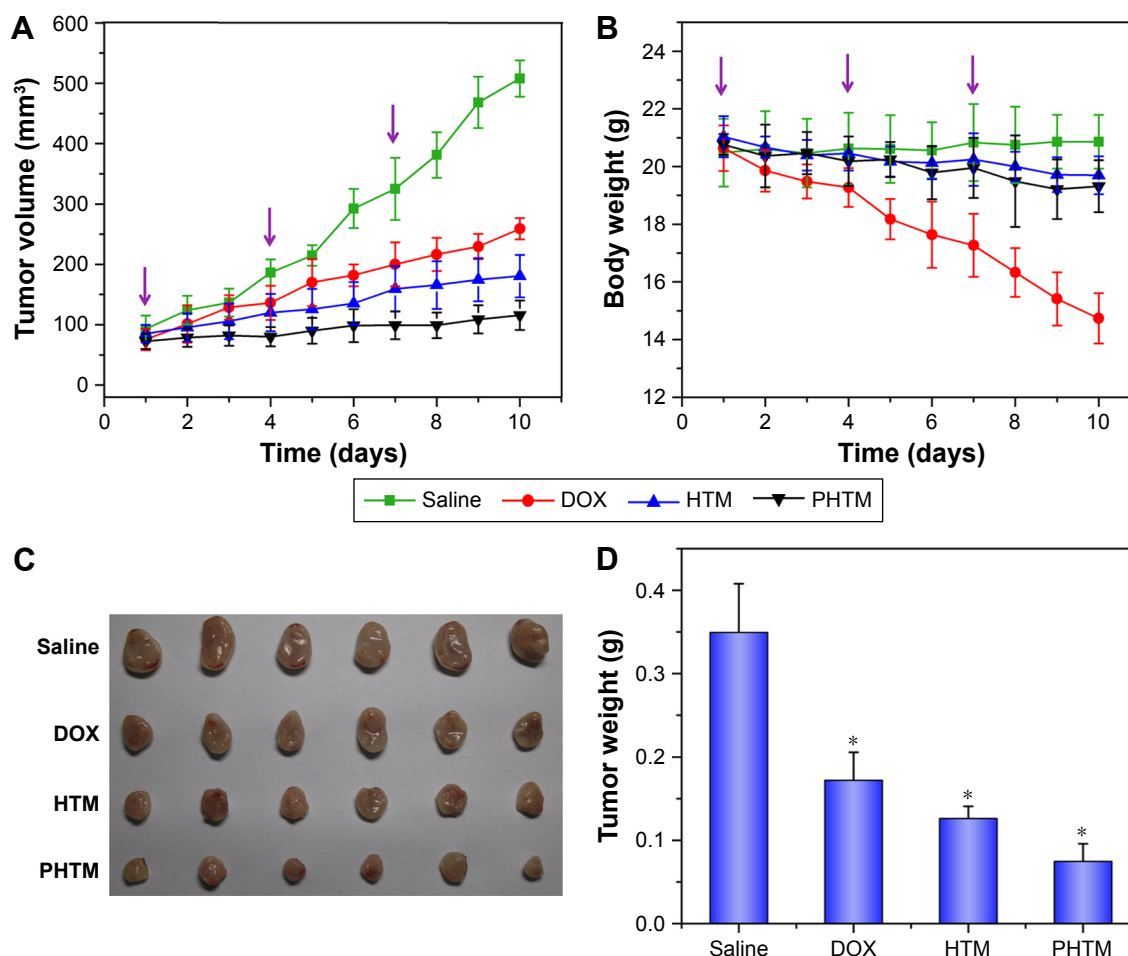
Figure 8 (**A**) The tumor volume and (**B**) body weight changes of saline, DOX solution, HTM, and PHTM on the MDA-MB-231 tumor-bearing mice; (**C**) the images of excised tumor tissues; and (**D**) the tumor weight of different formulation from MDA-MB-231 tumor-bearing mice at the time of sacrifice.
Notes: Data expressed as mean ± standard deviation (n=5). *$P<0.05$.
Abbreviations: DOX, doxorubicin; HA, hyaluronic acid; HTM, HA-PHis/TPGS2k mixed micelles; pep-TPGS2k, Her2 peptide-modified TPGS2k; PHis, poly(L-histidine); PHTM, HA-PHis/pep-TPGS2k mixed micelles; TPGS2k, d-α-tocopheryl polyethylene glycol 2000.

than that of HTM, respectively (Figure 8D). The results demonstrate that HA-based micelles decorated with Her2 peptide can significantly improve the antitumor efficacy. This enhanced tumor regression of PHTM is attributed to the synergy special recognition between the dual receptors and tumor cells.

Conclusion

Her2 peptide-modified pH-sensitive mixed micelles based on HA-PHis and TPGS2k copolymers were developed for precise targeted delivery of DOX into breast tumor cells. The PHTM exhibited high cytotoxicity and efficient internalization for MDA-MB-231 cells. Endocytosis inhibition studies revealed that the clathrin-/caveolae-mediated pathways were involved in the uptake of PHTM micelles. In vivo target and antitumor studies showed that PHTM could enhance the accumulation of anticancer drugs in the tumors and significantly inhibit the tumor growth. Therefore, PHTM can improve the

targeting ability of HA-based micelles and is a preferable active drug delivery carrier for cancer therapy.

Acknowledgment

Disclosure

The authors report no conflicts of interest in this work.

References

1. Chari RVJ. Targeted cancer therapy: conferring specificity to cytotoxic drugs. *Acc Chem Res*. 2008;41(1):98–107.
2. Hu Q, Gao X, Gu G, et al. Glioma therapy using tumor homing and penetrating peptide-functionalized PEG–PLA nanoparticles loaded with paclitaxel. *Biomaterials*. 2013;34(22):5640–5650.
3. Sakhrani NM, Padh H. Organelle targeting: third level of drug targeting. *Drug Des Devel Ther*. 2013;7:585.
4. Huang K, Ma H, Liu J, et al. Size-dependent localization and penetration of ultrasmall gold nanoparticles in cancer cells, multicellular spheroids, and tumors *in vivo*. *ACS Nano*. 2012;6(5):4483–4493.

5. Fang J, Nakamura H, Maeda H. The EPR effect: unique features of tumor blood vessels for drug delivery, factors involved, and limitations and augmentation of the effect. *Adv Drug Del Rev*. 2011;63(3):136–151.

6. Iyer AK, Khaled G, Fang J, Maeda H. Exploiting the enhanced permeability and retention effect for tumor targeting. *Drug Discov Today*. 2006;11(17):812–818.

7. Biswas S, Torchilin VP. Nanopreparations for organelle-specific delivery in cancer. *Adv Drug Del Rev*. 2014;66:26–41.

8. Bertrand N, Wu J, Xu X, Kamaly N, Farokhzad OC. Cancer nanotechnology: the impact of passive and active targeting in the era of modern cancer biology. *Adv Drug Del Rev*. 2014;66:2–25.

9. Peer D, Karp JM, Hong S, Farokhzad OC, Margalit R, Langer R. Nanocarriers as an emerging platform for cancer therapy. *Nat Nanotechnol*. 2007;2(12):751–760.

10. Byrne JD, Betancourt T, Brannon-Peppas L. Active targeting schemes for nanoparticle systems in cancer therapeutics. *Adv Drug Del Rev*. 2008;60(15):1615–1626.

11. Yu B, Tai HC, Xue W, Lee LJ, Lee RJ. Receptor-targeted nanocarriers for therapeutic delivery to cancer. *Mol Membr Biol*. 2010; 27(7):286–298.

12. des Rieux A, Pourcelle V, Cani PD, Marchand-Brynaert J, Préat V. Targeted nanoparticles with novel non-peptidic ligands for oral delivery. *Adv Drug Del Rev*. 2013;65(6):833–844.

13. Steinhauser IM, Langer K, Strebhardt KM, Spänkuch B. Effect of trastuzumab-modified antisense oligonucleotide-loaded human serum albumin nanoparticles prepared by heat denaturation. *Biomaterials*. 2008;29(29):4022–4028.

14. Sun B, Ranganathan B, Feng SS. Multifunctional poly (D, L-lactide-co-glycolide)/montmorillonite (PLGA/MMT) nanoparticles decorated by Trastuzumab for targeted chemotherapy of breast cancer. *Biomaterials*. 2008;29(4):475–486.

15. Binz HK, Amstutz P, Plückthun A. Engineering novel binding proteins from nonimmunoglobulin domains. *Nat Biotechnol*. 2005;23(10): 1257–1268.

16. Ruigrok Vincent JB, Levisson M, Eppink Michel HM, Smidt H, van der Oost J. Alternative affinity tools: more attractive than antibodies? *Biochem J*. 2011;436(1):1–13.

17. Bradbury AR, Sidhu S, Dübel S, McCafferty J. Beyond natural antibodies: the power of *in vitro* display technologies. *Nat Biotechnol*. 2011; 29(3):245–254.

18. Olivier GK, Cho A, Sanii B, Connolly MD, Tran H, Zuckermann RN. Antibody-mimetic peptoid nanosheets for molecular recognition. *ACS Nano*. 2013;7(10):9276–9286.

19. Shahin M, Ahmed S, Kaur K, Lavasanifar A. Decoration of polymeric micelles with cancer-specific peptide ligands for active targeting of paclitaxel. *Biomaterials*. 2011;32(22):5123–5133.

20. Awada A, Bozovic-Spasojevic I, Chow L. New therapies in HER2-positive breast cancer: a major step towards a cure of the disease? *Cancer Treat Rev*. 2012;38(5):494–504.

21. Shukla R, Thomas TP, Peters JL, et al. HER2 specific tumor targeting with dendrimer conjugated anti-HER2 mAb. *Bioconjug Chem*. 2006; 17(5):1109–1115.

22. Yousefpour P, Atyabi F, Vasheghani-Farahani E, Movahedi AA, Dinarvand R. Targeted delivery of doxorubicin-utilizing chitosan nanoparticles surface-functionalized with anti-Her2 trastuzumab. *Int J Nanomedicine*. 2011;6:1977–1990.

23. Tai W, Mahato R, Cheng K. The role of HER2 in cancer therapy and targeted drug delivery. *J Control Release*. 2010;146(3):264–275.

24. Kouchakzadeh H, Shojaosadati SA, Tahmasebi F, Shokri F. Optimization of an anti-HER2 monoclonal antibody targeted delivery system using PEGylated human serum albumin nanoparticles. *Int J Pharm*. 2013; 447(1):62–69.

25. Berezov A, Zhang HT, Greene MI, Murali R. Disabling erbB receptors with rationally designed exocyclic mimetics of antibodies: structure-function analysis. *J Med Chem*. 2001;44(16):2565–2574.

26. Jin YJ, Termsarasab U, Ko SH, et al. Hyaluronic acid derivative-based self-assembled nanoparticles for the treatment of melanoma. *Pharm Res*. 2012;29(12):3443–3454.

27. Choi KY, Yoon HY, Kim JH, et al. Smart nanocarrier based on PEGylated hyaluronic acid for cancer therapy. *ACS Nano*. 2011;5(11): 8591–8599.

28. Lee ES, Shin HJ, Na K, Bae YH. Poly (l-histidine)–PEG block copolymer micelles and pH-induced destabilization. *J Control Release*. 2003; 90(3):363–374.

29. Qiu L, Li Z, Qiao M, et al. Self-assembled pH-responsive hyaluronic acid–g-poly (l-histidine) copolymer micelles for targeted intracellular delivery of doxorubicin. *Acta Biomater*. 2014;10(5):2024–2035.

30. Qiu L, Qiao M, Chen Q, et al. Enhanced effect of pH-sensitive mixed copolymer micelles for overcoming multidrug resistance of doxorubicin. *Biomaterials*. 2014;35(37):9877–9887.

31. Aguiar DJ, Knudson W, Knudson CB. Internalization of the hyaluronan receptor CD44 by chondrocytes. *Exp Cell Res*. 1999;252(2):292–302.

32. Ouasti S, Kingham PJ, Terenghi G, Tirelli N. The CD44/integrins interplay and the significance of receptor binding and re-presentation in the uptake of RGD-functionalized hyaluronic acid. *Biomaterials*. 2012;33(4):1120–1134.

33. Choi KY, Saravanakumar G, Park JH, Park K. Hyaluronic acid-based nanocarriers for intracellular targeting: interfacial interactions with proteins in cancer. *Colloids Surf B Biointerfaces*. 2012;99:82–94.

34. Mochizuki S, Kano A, Shimada N, Maruyama A. Uptake of enzymatically-digested hyaluronan by liver endothelial cells in vivo and in vitro. *J Biomater Sci Polym Ed*. 2009;20(1):83–97.

35. Prevo R, Banerji S, Ferguson DJ, Clasper S, Jackson DG. Mouse LYVE-1 is an endocytic receptor for hyaluronan in lymphatic endothelium. *J Biol Chem*. 2001;276(22):19420–19430.

36. Arimoto J, Ikura Y, Suekane T, et al. Expression of LYVE-1 in sinusoidal endothelium is reduced in chronically inflamed human livers. *J Gastroenterol*. 2010;45(3):317–325.

37. Wright C, Angus B, Nicholson S, et al. Expression of c-erbB-2 oncoprotein: a prognostic indicator in human breast cancer. *Cancer Res*. 1989; 49(8):2087–2090.

38. Baselga J. Clinical trials of Herceptin® (trastuzumab). *Eur J Cancer*. 2001;37:18–24.

39. Dou S, Yao YD, Yang XZ, et al. Anti-Her2 single-chain antibody mediated DNMTs-siRNA delivery for targeted breast cancer therapy. *J Control Release*. 2012;161(3):875–883.

40. Li X, Ding L, Xu Y, Wang Y, Ping Q. Targeted delivery of doxorubicin using stealth liposomes modified with transferrin. *Int J Pharm*. 2009; 373(1):116–123.

41. Shi C, Gao F, Gao X, Liu Y. A novel anti-VEGF165 monoclonal antibody-conjugated liposomal nanocarrier system: physical characterization and cellular uptake evaluation in vitro and in vivo. *Biomed Pharmacother*. 2015;69:191–200.

42. Yin H, Lee ES, Kim D, Lee KH, Oh KT, Bae YH. Physicochemical characteristics of pH-sensitive poly (L-histidine)-b-poly (ethylene glycol)/poly (L-lactide)-b-poly (ethylene glycol) mixed micelles. *J Control Release*. 2008;126(2):130–138.

43. Luo Z, Jiang J. pH-sensitive drug loading/releasing in amphiphilic copolymer PAE–PEG: integrating molecular dynamics and dissipative particle dynamics simulations. *J Control Release*. 2012;162(1):185–193.

44. Johnson RP, Jeong YI, John JV, et al. Dual stimuli-responsive poly (N-isopropylacrylamide)-b-poly (L-histidine) chimeric materials for the controlled delivery of doxorubicin into liver carcinoma. *Biomacromolecules*. 2013;14(5):1434–1443.

45. Li J, Huo M, Wang J, et al. Redox-sensitive micelles self-assembled from amphiphilic hyaluronic acid-deoxycholic acid conjugates for targeted intracellular delivery of paclitaxel. *Biomaterials*. 2012;33(7): 2310–2320.

46. Cho HJ, Yoon IS, Yoon HY, et al. Polyethylene glycol-conjugated hyaluronic acid-ceramide self-assembled nanoparticles for targeted delivery of doxorubicin. *Biomaterials*. 2012;33(4):1190–1200.

47. Qiu L, Hu Q, Cheng L, et al. cRGDyK modified pH responsive nanoparticles for specific intracellular delivery of doxorubicin. *Acta Biomater*. 2016;30:285–298.

48. Liao LB, Zhou HY, Xiao XM. Spectroscopic and viscosity study of doxorubicin interaction with DNA. *J Mol Struct*. 2005;749(1):108–113.